

Evidence for a Spatially-Modulated Superfluid Phase of ^3He under Confinement

Lev V. Levitin,^{*} Ben Yager,[†] Laura Sumner,[‡] Brian Cowan, Andrew J. Casey, and John Saunders
Department of Physics, Royal Holloway University of London, Egham, Surrey, TW20 0EX, UK

Nikolay Zhelev,[§] Robert G. Bennett,[¶] and Jeevak M. Parpia
Department of Physics, Cornell University, Ithaca, NY, 14853 USA
(Dated: May 8, 2018)

In superfluid ^3He -B confined in a slab geometry, domain walls between regions of different order parameter orientation are predicted to be energetically stable. Formation of the spatially-modulated superfluid *stripe phase* has been proposed. We confined ^3He in a $1.1\ \mu\text{m}$ microfluidic cavity and cooled it into the B phase at low pressure, where the stripe phase is predicted. We measured the surface-induced order parameter distortion with NMR, sensitive to the formation of domains. The results rule out the stripe phase, but are consistent with two-dimensionally modulated superfluid order.

PACS numbers: 67.30.H-, 67.30.hr, 67.30.hj, 74.20.Rp

The pairing of fermions to form a superfluid or superconductor at sufficiently low temperatures is a relatively ubiquitous phenomenon. Examples include: electrically conducting systems from metals to organic materials to metallic oxides; neutral atoms from ^3He to ultracold fermionic gases; and astrophysical objects such as neutron stars and pulsars. In the most straightforward case the pairs form a macroscopic quantum condensate which is spatially uniform. In type-II superconductors a spatially inhomogeneous state, the Abrikosov flux lattice, arises in a magnetic field. Its origin is the negative surface energy between normal and superconducting regions. On the other hand the realization and experimental identification of states with spatially modulated superfluid/superconducting order has proved challenging.

The Fulde-Ferrell-Larkin-Ovchinnikov (FFLO) state [1, 2], has been predicted to arise in *spin-singlet* superconductors. An imbalance between spin-up and spin-down Fermi momenta, driven by ferromagnetic interactions or high magnetic fields, induces pairing with non-zero centre of mass momentum. This results in both the order parameter and the spin density oscillating in space with the same wavevector. The FFLO state is predicted to intervene beyond the Pauli limiting field, inhibiting the destruction of superconductivity [3]. It requires orbital effects to be weak, restricting possible materials for its observation. There is evidence of the FFLO state in the low-dimensional organic superconductor κ -(BEDT-TTF) $_2\text{Cu}(\text{NCS})_2$ [4, 5]. Previously identified as FFLO [6], a more complex state, with intertwined p-wave pair density wave (PDW) and spin density wave has been proposed in the heavy fermion d-wave superconductor CeCoIn_5 [7–9]. Elsewhere a PDW commensurate with a charge density wave, has been clearly demonstrated in the d-wave cuprate superconductor $\text{Bi}_2\text{Sr}_2\text{CaCu}_2\text{O}_{8+x}$ [10]. In the ultracold fermionic gas ^6Li , superfluidity with imbalanced spin populations has been observed [11] with thermodynamic evidence consistent with FFLO [12]. In

addition to these condensed matter systems it has been proposed that quantum chromodynamics may provide a pathway to inhomogeneous superconductivity, potentially realised in astrophysical objects [13].

In general the order parameter modulation is expected to be more complex than the model FFLO state [3, 14]. Potential examples are: 1D domain walls of thickness much smaller than the width of domains; 2D modulated structures, involving multiple wavevectors [3]. Furthermore, nucleation barriers and metastability may inhibit the formation of periodic states [14].

In this paper we report experimental investigation of a predicted spatially modulated state in the topological p-wave, *spin-triplet*, superfluid ^3He [15]. This requires the superfluid to be confined in a thin cavity of uniform thickness. At the heart of this predicted stripe phase is the stabilization of a hard domain wall, of thickness comparable to the superfluid coherence length, in superfluid ^3He -B under confinement in a slab geometry. These B-B domain walls were first classified in [16], and the analogy drawn with cosmic domain walls. Their stability in the bulk, and possible evidence for their observation is discussed in [17]. Under confinement the presence of the domain wall reduces surface pair-breaking, and can result in a negative surface energy of the domain wall, leading to formation of a stripe phase [15, 18, 19].

In superfluid ^3He the nuclear spins constitute the spin part of the pair wavefunction; thus nuclear magnetic resonance (NMR) is widely used to provide a direct fingerprint of the superfluid order parameter [20, 21]. NMR has been predicted to distinguish clearly between the striped and translationally-invariant states of the B phase [18, 22].

To optimise the formation of stripes in this work we chose a slab geometry of height $D = 1.1\ \mu\text{m}$, where the B phase is stable down to zero pressure [23]. The stripe phase was originally predicted in the weak-coupling limit of BCS theory [15], while the strong-coupling corrections

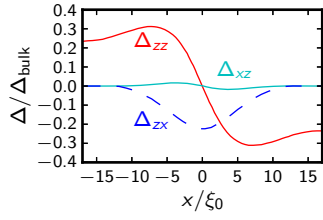


FIG. 1. Domain wall at the heart of the stripe phase in ${}^3\text{He-B}$ [15]. Shown here are the elements of the energy gap matrix Δ , such that $\mathbf{A} = e^{i\phi}\mathbf{R}\Delta$. In (1) $\Delta = \text{diag}(\Delta_{\parallel}, \Delta_{\parallel}, \Delta_{\perp})$. Crossing the domain wall lying in yz -plane at $x = 0$, Δ_{zz} changes from Δ_{\perp} to $-\Delta_{\perp}$, and off-diagonal elements Δ_{xz} and Δ_{zx} emerge, while Δ_{xx} and Δ_{yy} (not shown) remain close to Δ_{\parallel} . The gap amplitudes were calculated at $z = 2.5\xi_0$ away from one of the walls in a $D = 10\xi_0$ thick slab at $T = 0.5T_c^{\text{bulk}}$; ξ_0 is the Cooper pair diameter, Δ_{bulk} is the bulk B phase gap.

to this theory in general favour the A phase and suppress the stability of stripes [18]. At present the strong coupling effects are not fully understood theoretically, leaving the stability of the stripe phase an open question [18, 23]. We performed the experiment at low pressure to minimise the strong-coupling effects.

Here we show that under our experimental conditions the stripe phase is clearly ruled out. However, there is NMR evidence for a spatially modulated superfluid of two-dimensional morphology, similar to states discussed in the context of FFLO [3]; we term this *polka-dot*.

The 3×3 matrix order parameter of a p-wave superfluid ${}^3\text{He}$ allows for multiple superfluid phases with different broken symmetries and topological invariants [20, 21]. In the bulk, at low pressure and magnetic field the stable state is the quasi-isotropic B phase with order parameter matrix $\mathbf{A} = e^{i\phi}\mathbf{R}\Delta$, where Δ is the energy gap, isotropic in the momentum space, ϕ is the superfluid phase and $\mathbf{R} = \mathbf{R}(\hat{\mathbf{n}}, \theta)$ is the matrix of relative spin-orbit rotation, parametrised by angle θ and axis $\hat{\mathbf{n}}$. This quasi-isotropic phase is relatively easily distorted by magnetic field or flow. Under confinement the distortion is strong and spatially inhomogeneous, induced by surface pair-breaking. In a slab normal to the z -axis, the order parameter is predicted to take the form

$$\mathbf{A}(z) = e^{i\phi}\mathbf{R} \begin{pmatrix} \Delta_{\parallel}(z) & & \\ & \Delta_{\parallel}(z) & \\ & & \Delta_{\perp}(z) \end{pmatrix}, \quad (1)$$

with $0 \leq \Delta_{\perp} < \Delta_{\parallel}$ due to stronger surface pair-breaking of Cooper pairs with orbital momentum parallel to the wall [24]. This distortion is named *planar* after the planar phase, in which $\Delta_{\perp} = 0$ [21].

The order parameter (1) has a large manifold of orientations, determined by ϕ , $\hat{\mathbf{n}}$ and θ , allowing domain walls between regions of different orientations [16, 17]. Domain

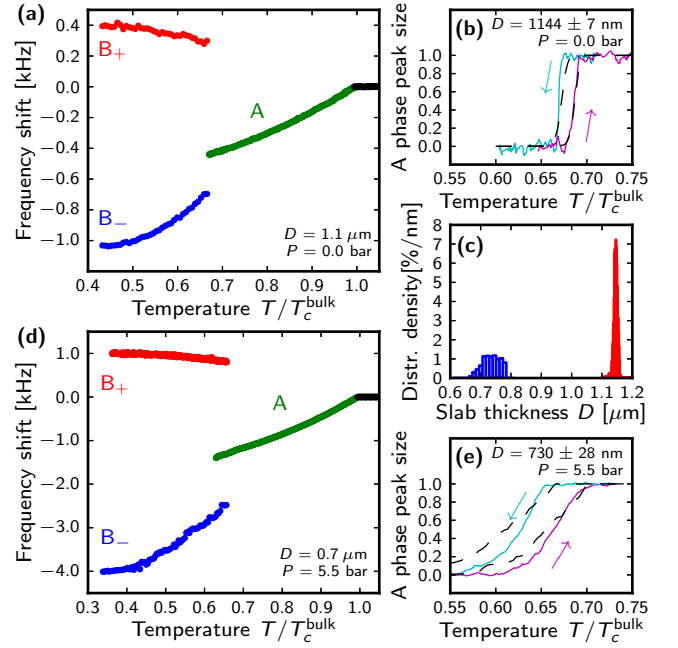


FIG. 2. Small tipping angle NMR signatures of A and B phases in $D = 1.1 \mu\text{m}$ slab (this work) (a,b) compared to the qualitatively similar measurements in $D = 0.7 \mu\text{m}$ slab (d,e) [28]. At the second-order normal-superfluid transition a negative frequency shift develops as the slab enters the A phase with the dipole-unlocked orientation. On further cooling a first-order phase transition into the B phase with a planar distortion occurs, where two possible states B_+ and B_- are observed. On warming from the B phase, the A phase fills the cell gradually (vice versa on cooling) in reasonable agreement with the transition occurring at a constant reduced thickness D/ξ (dashed black lines) [23] in the presence of variation of D across the cell, measured with optical interferometry (c). The hysteresis between cooling and warming is attributed to pinning of the AB interface.

walls where Δ_{\perp} changes sign,

$$e^{i\phi}\mathbf{R} \begin{pmatrix} \Delta_{\parallel} & & \\ & \Delta_{\parallel} & \\ & & \Delta_{\perp} \end{pmatrix} \quad \Bigg| \quad e^{i\phi}\mathbf{R} \begin{pmatrix} \Delta_{\parallel} & & \\ & \Delta_{\parallel} & \\ & & -\Delta_{\perp} \end{pmatrix},$$

are predicted to have negative surface energy in the B phase confined in a slab, close to the A-B transition [15, 25], see Fig. 1. As a consequence the slab of ${}^3\text{He-B}$ would spontaneously break into domains, until the domain walls get close enough that their mutual repulsion becomes significant. This is predicted to result in a periodic *stripe phase* with a typical domain size W of order D [15, 18, 19]. Phases with spontaneously broken translational invariance are also predicted to stabilise in ${}^3\text{He}$ confined to narrow pores [26, 27].

In this experiment we performed pulsed NMR studies on a slab of ${}^3\text{He}$ confined in a $D = 1144 \pm 7 \text{ nm}$ thick silicon-glass microfluidic cavity, in a field of 31 mT perpendicular to the slab (corresponding to ${}^3\text{He}$ Larmor

frequency $f_L = 1.02$ MHz), using the setup described in Ref. [28]. An additional support structure was introduced [29] which significantly improved the homogeneity of the cavity height, Fig. 2c. The measurements were performed at low pressure $P = 0.03$ bar, where the bulk superfluid transition temperature $T_c^{\text{bulk}} = 0.93$ mK, and close to specular scattering, achieved by preplating the cell walls with a $64 \mu\text{mol}/\text{m}^2$ (~ 5 atomic layers) ^4He film. To avoid gradual depletion of the ^4He film due to the fountain effect the cell fill line was interrupted with a superfluid-leaktight cryogenic valve at 6 mK [30].

We first mapped the phase diagram with small tipping angle, $\beta = 4^\circ$, NMR pulses, Fig. 2a,b. The A-B transition was observed at $T_{\text{AB}} = 0.7T_c^{\text{bulk}}$ in agreement with torsional oscillator measurements, with a 1080 nm cavity [23]. As we previously observed in the $0.7 \mu\text{m}$ cavity, the B phase nucleated stochastically in two spin-orbit orientations with distinct NMR signatures: stable B_+ and metastable B_- [22]. For comparison Fig. 2d,e shows similar A-B transition signatures from the $D = 0.7 \mu\text{m}$ slab at higher pressure. The significantly improved width of the transition is evident. On the other hand, for both cavities we observe hysteresis between A to B and B to A transitions. We attribute this to the pinning of the AB interface at scratches on the glass wall of the sample cell since, by contrast, the A-B transition was found to be reversible in the torsional oscillator with improved surface quality [23].

The magnitudes of the frequency shifts of translationally invariant B_+ and B_- , Δf_+ and Δf_- , are determined by averages of the gap structure across the cavity [22]: $\langle \Delta_{\parallel}^2 \rangle$, $\langle \Delta_{\parallel} \Delta_{\perp} \rangle$ and $\langle \Delta_{\perp}^2 \rangle$. In the case of a spatially modulated phase, we must also average in the plane of the cavity to determine the NMR response. This procedure is valid when the width of the stripes W is smaller than the dipole length $\xi_D \sim 10 \mu\text{m}$ [22], a condition predicted to hold for this cavity ($W \approx D\sqrt{3} \ll \xi_D$) except very close to the stripe-to-B transition [18]. In the stripe phase $\langle \Delta_{\parallel} \Delta_{\perp} \rangle = 0$ due to Δ_{\perp} having opposite sign in the adjacent domains [22], and this has clear signatures in the NMR response, as a function of tipping angle.

We define the dimensionless gap distortion parameters

$$\bar{q} = \langle \Delta_{\parallel} \Delta_{\perp} \rangle / \langle \Delta_{\parallel}^2 \rangle, \quad \bar{Q} = \sqrt{\langle \Delta_{\perp}^2 \rangle / \langle \Delta_{\parallel}^2 \rangle}. \quad (2)$$

The tipping angle dependence of the frequency shift of B_+ , below the so called ‘‘magic angle’’, $\beta^* > 104^\circ$, scaled by the small-tipping-angle shift of B_- is given by [22]

$$\frac{\Delta f_+(\beta \rightarrow 0)}{\Delta f_-(\beta \rightarrow 0)} = \frac{2\bar{Q}^2 - \bar{q}^2 - 1}{1 + 2\bar{Q}^2}, \quad (3a)$$

$$\frac{\partial \Delta f_+(\beta) / \partial \cos \beta}{\Delta f_-(\beta \rightarrow 0)} = \frac{2\bar{Q}^2 - 2\bar{q}^2}{1 + 2\bar{Q}^2}, \quad (3b)$$

where β is the tip angle. We further note that: $\Delta f_-(\beta)$ does not depend on \bar{q} ; the magic angle at which there is

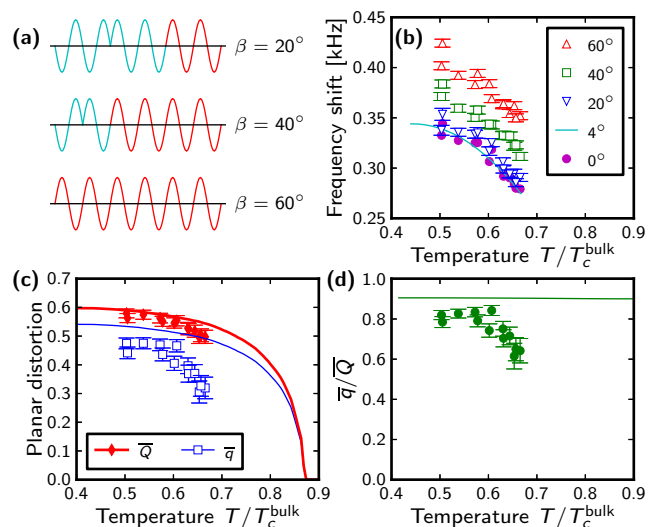


FIG. 3. NMR measurement of the planar distortion \bar{q} , \bar{Q} as a function of temperature. (a) Technique for applying a set of pulses with different tipping angle β but equal heating: all pulses coincide in length and amplitude; β is reduced by applying the initial section of the pulse with a 180° phase shift, which cancels out a similar section that follows (both light blue), so only the remainder of the pulse (red) tips the spins. (b) Initial frequency shifts in B_+ after such pulses yield $\partial \Delta f_+ / \partial \cos \beta$ and $\Delta f_+(\beta \rightarrow 0)$. Good agreement between $\Delta f_+(\beta \rightarrow 0)$ obtained here and $\Delta f_+(4^\circ)$, smoothed from Fig. 2a, indicates that heating due to the pulses used here is negligible. (c,d) Temperature dependence of planar distortion parameters \bar{q} , \bar{Q} and \bar{q}/\bar{Q} inferred from (b) and $\Delta f_-(4^\circ)$, Fig. 2a. Solid lines show weak-coupling calculations for translationally-invariant B phase [31]. In the absence of strong coupling, the AB transition would occur at a higher temperature than observed. We find \bar{Q} in agreement with the theory, while \bar{q} is reduced.

a kink in $\Delta f_+(\beta)$ is given by $\beta^* = \arccos(\bar{q} - 2)/(2\bar{q} + 2)$ [22]. Thus there is no magic angle expected for the stripe phase, for which $\bar{q} = 0$.

Our experiments were restricted to modest tipping angles, due to heating of the ^3He , induced by large NMR tipping pulses, via an unidentified mechanism within the microfluidic cavity. Therefore we focussed on measuring $\Delta f_+(\beta)$ below the magic angle β^* approaching as close as possible to the AB transition. We developed a scheme for applying different β pulses while inducing identical heating, shown in Fig. 3a. Triplets of such pulses with $\beta = 20^\circ$ to 60° were applied during step-wise temperature ramps. We inferred $\partial \Delta f_+ / \partial \cos \beta$ and $\Delta f_+(\beta \rightarrow 0)$ from the data shown in Fig. 3b and confirmed the heating effects to be negligible for these pulses. Combining with $\Delta f_-(\beta \rightarrow 0)$ at the same temperature, Fig. 2a, we determine the planar distortion parameters \bar{q} and \bar{Q} through (3), shown in Fig. 3c.

In the above analysis the off-diagonal elements of the gap matrix near domain walls (see Fig. 1) have been ne-

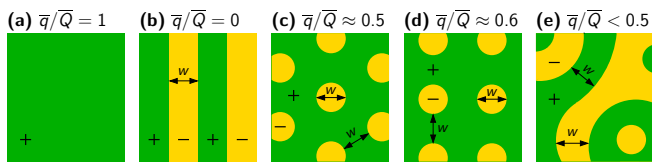


FIG. 4. Possible domain configurations in ${}^3\text{He-B}$ confined to a slab, view perpendicular to the slab plane. $+/-$ indicates the sign of Δ_{\perp} . (a) translationally-invariant B phase, (b) predicted regular stripe phase, (c,d) proposed regular polka dot phase that is easier to nucleate than the stripe phase, (e) disordered array of circular domains that may arise if dots have a chance to expand before getting within reach of each other, leading to less imbalance between $+$ and $-$ regions than (c,d). The values of the gap distortion parameter \bar{q}/\bar{Q} are derived under a simplified assumption of step-like domain walls. All features in (c-e) are taken to be of characteristic size similar to the pitch W of the stripe phase

glected. Incorporating the detailed gap structure at the domain walls into the NMR model leaves the signature of the stripe phase, $\bar{q} = 0, \bar{Q} > 0$, virtually unchanged [18]. We can therefore conclude unambiguously that the stripe phase was not present in our experiment.

Nevertheless, the measured \bar{q} is reduced compared to the weak-coupling calculations for the translationally-invariant B phase [31], see Fig. 3c,d. This contrasts with the good agreement between these calculations and similar measurements in a $D = 0.7 \mu\text{m}$ slab at higher pressure [22]. We therefore consider domain structures in which the amount a and $1-a$ of domains with positive and negative Δ_{\perp} is unequal. For a qualitative estimate we will assume that the domain walls are step-like and ignore gap variation across the slab, $\Delta_{\parallel} = \text{const}, |\Delta_{\perp}| = \text{const}$. Then

$$\bar{Q} = \frac{|\Delta_{\perp}|}{\Delta_{\parallel}}, \quad \bar{q} = (2a - 1) \frac{|\Delta_{\perp}|}{\Delta_{\parallel}}, \quad \frac{\bar{q}}{\bar{Q}} = 2a - 1. \quad (4)$$

Since the sign of Δ_{\perp} can be flipped with a rotation [25], we only need to consider a situation where the larger part of the slab has positive Δ_{\perp} , $a \geq 0.5$, so $\bar{q} \geq 0$ as required in (3) [22]. The gradual variation of Δ_{\parallel} , Δ_{\perp} and the emergence of the off-diagonal gap matrix elements inside the domain walls would lead to corrections to this model that should be taken into account in future theoretical work.

Our measurement $\bar{q}/\bar{Q} \approx 0.6$ near the T_{AB} suggests the $+/-$ domain population of 3 : 1. A likely scenario for imbalance of domains is a two-dimensional structure. Possible morphologies are illustrated in Fig. 4, suggesting we might have observed a regular *polka dot phase* with hexagonal or square symmetry, Fig. 4c,d.

Such structures may be stabilised by energetic considerations, requiring further theoretical work. On the other hand they may arise because of a lower nucleation barrier for “dots” compared to stripes, which are macroscopic in

one dimension. The regular lattice of “dots” may form if the neighbouring dots nucleate rapidly enough to prevent each one from growing beyond typical size W before getting within W of the others. It is also possible that curved domain walls are energetically favoured over straight ones, preventing the dots from expansion beyond some equilibrium diameter W' , which may differ from the equilibrium separation between the dots W . The increase of \bar{q}/\bar{Q} on cooling may indicate a different temperature dependence of W and W' .

In conclusion, in the search for the predicted spatially modulated superfluid “stripe phase” of ${}^3\text{He}$ we have cooled a $1.1 \mu\text{m}$ -thick slab of ${}^3\text{He}$ into the superfluid B phase at low pressure, as close as possible to the weak coupling limit. We have measured the degree of planar distortion as a function of temperature up to the AB transition. The predicted clear signature of the stripe phase was not observed. Nevertheless, disagreement was found between our data and the theoretically calculated planar distortion of the translationally-invariant B phase. This leads us to propose a superfluid phase with two-dimensional spatial modulation.

In view of this result, experiments to detect the stripe phase by studies of in-plane anisotropy, for example in thermal transport, should be approached with caution. Future NMR experiments should study the pressure dependence of the planar-distorted the confined B phase, since the stripes are predicted to be destabilized by strong coupling effects above a certain pressure [18]. Another signature may be a dramatic increase in the metastability of the A phase above this pressure [23]. The precise measurement of the “magic angle” in pulsed NMR is a further objective, requiring optimizing the microfluidic cavities to eliminate heating. ${}^3\text{He}$ confined in a well-defined slab geometry at constant density/chemical potential and with no impurities appears to provide a highly promising model system for the study of putative spontaneous spatially-modulated superfluidity.

We thank B. R. Ilic for help with microfluidic chamber fabrication and design methodology; A. Vorontsov and J. Sauls for sharing calculations of the gap profile of confined ${}^3\text{He}$. This work was supported by EPSRC grant EP/J022004/1; NSF grants DMR-1202991 and DMR-1708341, and the European Microkelvin Platform.

* l.v.levitin@rhul.ac.uk

† Now at Institute for Quantum Computing, University of Waterloo, Waterloo, Ontario N2L 3G1, Canada

‡ Now at Imperial College London, London SW7 2AZ, UK

§ Now at Corning Incorporated, USA

¶ Now at Vantage Power Ltd, London, UB6 0FD, UK

[1] A. I. Larkin and Yu. N. Ovchinnikov, Sov. Phys. JETP **20**, 762 (1965).

[2] P. Fulde and R. A. Ferrell, Phys. Rev. A **135**, 550 (1964).

- [3] Y. Matsuda and H. Shimahara, *J. Phys. Soc. Jpn* **76**, 051005 (2007).
- [4] H. Mayaffre, S. Krämer, M. Horvatić, C. Berthier, K. Miyagawa, K. Kanoda, and V. F. Mitrović, *Nat. Phys.* **10**, 928 (2014).
- [5] C. Agosta, N. A. Fortune, S. T. Hannahs, S. Gu, L. Liang, J.-H. Park, and J. A. Schleuter, *Phys. Rev. Lett.* **118**, 267001 (2017).
- [6] A. Bianchi, R. Movshovich, C. Capan, P. G. Pagliuso, and J. L. Sarrao, *Phys. Rev. Lett.* **91**, 187004 (2003).
- [7] G. Koutroulakis, M. D. Stewart, Jr., V. F. Mitrović, M. Horvatić, C. Berthier, G. Lapertot, and J. Flouquet, *Phys. Rev. Lett.* **104**, 087001 (2010).
- [8] D. K. Kim, S.-Z. Lin, F. Weickert, M. Kenzelmann, E. D. Bauer, F. Ronning, J. D. Thompson, and R. Movshovich, *Phys. Rev. X* **6**, 041059 (2016).
- [9] D. Y. Kim, S.-Z. Lin, F. Weickert, E. D. Bauer, F. Ronning, J. D. Thompson, and R. Movshovich, *Phys. Rev. Lett.* **118**, 197001 (2017).
- [10] M. H. Hamidian, S. D. Edkins, S. H. Joo, A. Kostin, H. Eisaki, S. Uchida, M.J. Lawler, E.-A. Kim, A.P. Mackenzie, K. Fujita, J. Lee, and J. C. Séamus Davis, *Nature* **532**, 343 (2016).
- [11] M. W. Zwierlein, A. Schirotzek, C. H. Schunck, and W. Ketterle, *Science*, **311**, 492 (2006).
- [12] M. C. Revelle, J. A. Fry, B. A. Olsen, and R. G. Hulet, *Phys. Rev. Lett.* **117**, (2016).
- [13] R. Casalbuoni and G. Nardulli, *Rev. Mod. Phys.* **76**, 263 (2004).
- [14] S. Dutta and E. Mueller, *Phys. Rev. A* **96**, 023612 (2017).
- [15] A. B. Vorontsov and J. A. Sauls, *Phys. Rev. Lett.* **98**, 045301 (2007), *J. Low Temp. Phys.* **138**, 283 (2005).
- [16] M.M. Salomaa and G.E. Volovik, *Phys. Rev. B* **37**, 9298 (1988).
- [17] M. Silveri, T. Turunen, E. Thuneberg, *Phys. Rev. B* **90**, 184513 (2014).
- [18] J. J. Wiman and J. A. Sauls, *J. Low Temp. Phys.* **184**, 1054 (2016).
- [19] K. Aoyama, *J. Phys. Soc. Jpn.* **85**, 094604 (2016).
- [20] A. J. Leggett, *Rev. Mod. Phys.* **47**, 332 (1975).
- [21] D. Vollhardt and P. Wolfe, *The superfluid phases of ^3He* , Taylor and Francis (1990).
- [22] L. V. Levitin, R. G. Bennett, E. V. Surovtsev, J. M. Parpia, B. Cowan, A. Casey, J. Saunders, *Phys. Rev. Lett.* **111**, 235304 (2013).
- [23] N. Zhelev, T. S. Abhilash, E. N. Smith, R. G. Bennett, X. Rojas, L. Levitin, J. Saunders, J. M. Parpia, *Nat. Comm.* **8**, 15963 (2017).
- [24] Y. Nagato, K. Nagai, *Physica B* **284-288**, 269 (2000).
- [25] Note that the state with $\Delta_{\perp} < 0$ on the right of the domain wall in Fig. 1 can be written in the canonical form (1) with $\Delta_{\perp} > 0$ using a π phase shift and a combined rotation $\mathbf{R}(\hat{\mathbf{n}}', \theta') = \mathbf{R}(\hat{\mathbf{n}}, \theta)\mathbf{R}(\hat{\mathbf{z}}, \pi)$:
- $$e^{i\phi}\mathbf{R}(\hat{\mathbf{n}}, \theta) \begin{pmatrix} \Delta_{\parallel} & & \\ & \Delta_{\parallel} & \\ & & -\Delta_{\perp} \end{pmatrix} = -e^{i\phi}\mathbf{R}(\hat{\mathbf{n}}, \theta) \begin{pmatrix} -\Delta_{\parallel} & & \\ & -\Delta_{\parallel} & \\ & & \Delta_{\perp} \end{pmatrix} \\ = e^{i(\phi+\pi)}\mathbf{R}(\hat{\mathbf{n}}, \theta)\mathbf{R}(\hat{\mathbf{z}}, \pi) \begin{pmatrix} \Delta_{\parallel} & & \\ & \Delta_{\parallel} & \\ & & \Delta_{\perp} \end{pmatrix}.$$
- [26] K. Aoyama, *Phys. Rev. B* **89**, 140502R (2014).
- [27] J.J. Wiman and J.A. Sauls, arXiv:1802.08719 (2018)
- [28] L. V. Levitin, R. G. Bennett, A. Casey, B. Cowan, J. Saunders, D. Drung, Th. Schurig, J. M. Parpia, *Science* **340**, 841 (2013).
- [29] N. Zhelev, T. S. Abhilash, R. G. Bennett, E. N. Smith, B. R. Ilic, J. M. Parpia, L. V. Levitin, X. Rojas, A. Casey, J. Saunders, arXiv:1805.00958.
- [30] V. Dotsenko and N. Mulders. *J. Low Temp. Phys.* **134**, 443 (2004).
- [31] A. B. Vorontsov and J. A. Sauls, *Phys. Rev. B* **68**, 064508 (2003) and private communication.